New developments in high pressure x-ray spectroscopy beamline at High Pressure Collaborative Access Team

Y. M. Xiao, P. Chow, G. Boman, L. G. Bai, E. Rod, A. Bommannavar, C. Kenney-Benson, S. Sinogeikin, and G. Y. Shen

---

New developments in high pressure x-ray spectroscopy beamline at High Pressure Collaborative Access Team

Y. M. Xiao,[a)] P. Chow, G. Boman, L. G. Bai, E. Rod, A. Bommannavar, C. Kenney-Benson, S. Sinogeikin, and G. Y. Shen

HPCAT, Geophysical Laboratory, Carnegie Institution of Washington, 9700 South Cass Avenue, Argonne, Illinois 60439, USA

The 16 ID-D (Insertion Device - D station) beamline of the High Pressure Collaborative Access Team at the Advanced Photon Source is dedicated to high pressure research using X-ray spectroscopy techniques typically integrated with diamond anvil cells. The beamline provides X-rays of 4.5-37 keV, and current available techniques include X-ray emission spectroscopy, inelastic X-ray scattering, and nuclear resonant scattering. The recent developments include a canted undulator upgrade, 17-element analyzer array for inelastic X-ray scattering, and an emission spectrometer using a polycapillary half-lens. Recent development projects and future prospects are also discussed. © 2015 AIP Publishing LLC. [http://dx.doi.org/10.1063/1.4926888]

I. INTRODUCTION

The behavior of materials under high pressure attracts scientists from various fields such as physics, chemistry, materials science, and earth and planetary sciences.[1–3] Some techniques, such as optical Raman spectroscopy, X-ray diffraction (XRD), and X-ray absorption spectroscopy (XAS), have been used for high pressure research for decades.[4,5] Thanks to the continuous developments of extremely intense and focused X-ray beams, together with the developments in high pressure vessels such as the X-ray transparent gasket and panoramic diamond anvil cells (DACs) with large opening angles, many X-ray spectroscopic methods (emission, inelastic scattering, nuclear resonant scattering (NRS), and magnetic circular dichroism) have become available for high pressure research since middle 1990s.[6–10] Since the beginning of user operation in 2002, the 16-ID-D beamline of the High Pressure Collaborative Access Team (HPCAT) at the Advanced Photon Source (APS) has been dedicated to high pressure spectroscopic studies, typically in DACs.[11] Current available techniques include X-ray emission spectroscopy (XES), inelastic X-ray scattering (IXS), and NRS. These techniques have been developed to meet the requirements in high pressure experiments. First of all, the sample ranges from a few micrometers to a couple of hundred micrometers at most in diameter in a DAC depending on the target pressure of the experiment. The sample thickness usually is even smaller, ranging from a few micrometers to a few tens of micrometers. To get acceptable signal-to-noise ratios with such small samples, a small focused beam becomes necessary for high pressure beamlines. At HPCAT, we use two sets of Kirkpatrick-Baez (KB) mirrors or combinations of these two sets to get an optimized beam size and flux for individual experiments. Second, in order to achieve high pressure conditions, the sample is always surrounded by other materials such as gaskets, anvils, and the pressure medium. These surrounding materials not only make sample access difficult, thus causing difficulties for some measurements like resistivity and magnetism under high pressure, but also generate background noise, especially for high pressure x-ray spectroscopy experiments because sample volume is several orders of magnitude smaller than those of gaskets and anvils. Post-sample collimation is thus critical for these experiments. At HPCAT, tweezers slit which can be put a few millimeters away from sample is used in most cases and a confocal optic, like a full polycapillary, is used as well.[12]

In this paper, we describe the capabilities and unique features of the spectroscopy beamline optimized for high pressure research, together with some recent developments and future prospects. A summary of the beamline capabilities is listed in Table I.

II. BEAMLINE OVERVIEW

The X-ray beam is provided by a single 2.1 m long undulator with a magnetic period of 30 mm. A schematic layout of the beamline is shown in Figure 1. The beamline consists of three end-stations: 16 ID-A, 16 ID-C, and 16 ID-D. A set of water-cooled white-beam slits and a liquid nitrogen cooled Si (1 1 1) double crystal monochromator (DCM, from Bruker) are located in 16 ID-A. The white-beam slits are ~25 m away from the source and their sizes are kept at 1 mm (V) × 1.5 mm (H) accepting the full undulator beam. The liquid N_2 cooled Si DCM is placed at ~27 m from the source, providing X-rays from 4.5 keV up to 37 keV with a fixed vertical offset of 25 mm. The second crystal of the Si DCM is 270 mm long and does not require translation along the beam during energy change, thus enhancing the stability during energy change. In addition, there is a piezoelectric actuator mounted on the second crystal which can be used for beam position stabilization through a feedback system. 16 ID-C houses a set of slits, high resolution monochromator (HRM) for ^{57}Fe NRS experiments, and a pair of long KB mirrors (Seso). The mirrors are 1 m and 1.2 m in the vertical and horizontal directions, respectively. To minimize switching-time between different

a)yxiao@carnegiescience.edu

86, 072206-1

TABLE I. Beamline summary.

Source	Single APS undulator 3.0
Monochromator	Bruker liquid N_2 cooled Si(1 1 1)
Energy range	4.5-37 keV
Beam size and focusing optics	30 (V) × 50 (H) μm with 1 m long KB mirrors 3 (V) × 5 (H) μm with 200 mm long KB mirrors or combine 1 long KB mirror with 1 short KB mirror
Flux at sample position	NRS: ~1×10^9 ph/s, 2 meV energy solution at 14.4 keV Others: ~5×10^{12} ph/s at 10 keV flux based on using 1 m long KB mirrors
Established techniques	Nuclear resonant scattering (2 meV for ^{57}Fe, LT down to ~4 K for NFS, *in-situ* XRD) Inelastic X-ray scattering/X-ray Raman scattering (~1 eV energy resolution) Resonance/X-ray emission Spectroscopy (~1 eV energy resolution, LT down to ~10 K, *in-situ* XRD)
Detectors	100K Pilatus detector, avalanche photo diode (APD), AmpTek, MarCCD
Support equipment	Cryostats for XES and NFS, online Ruby system, membrane cell control, external heating

experiments and keep the focus spot at the same position, the vertical KB mirror angle is fixed at 2 mrad except for NRS experiments, for which 1mrad is used due to a 77 mm offset in the vertical direction induced by the HRM; the horizontal KB mirror angle is normally set at 3 mrad. Both KB mirrors have three coating stripes, Si, Pt, and Pd, to cover the wide energy range. The KB mirrors are located approximately 4.5 m (horizontal) and 5.5 m (vertical) upstream of the sample stage in 16-ID-D. The typical focus spot at the sample position is ~30 (V) × 50 (H) μm^2 at full width at half maximum (FWHM) with a flux of ~5×10^{12} photon/s at 10 keV. 16 ID-D is the experimental station which consists of a set of sample stages, a dedicated XES and a 2.7 m horizontal arm which can be rotated from 0° to 90° for IXS experiments. The sample stages include a rotation stage, a tilt stage, and fine x-y-z translational stages with large range to accommodate precise mounting for a variety of sample environments such as furnace and cryostat. A pair of 200 mm long KB mirrors which are located 0.3-0.5 m away from sample position can be setup to focus the beam down to 3 (V) × 5(H) μm^2 with ~20% flux relative to the beam using the long KB mirrors. In Figure 2, using combinations of mirrors to satisfy the various experimental requirements, all available focus profiles at the sample position including sharp edge scans for the 3 (V) × 5(H) μm^2 focus are shown. During long repeating DCM energy scans, the focus beam position can be shifted to ~1-2 μm.

III. HIGH PRESSURE X-RAY SPECTROSCOPY TECHNIQUES

A. High pressure x-ray emission spectroscopy

XES is a photon-in-photon-out process. During the process, a core electron is excited by the incident X-ray and
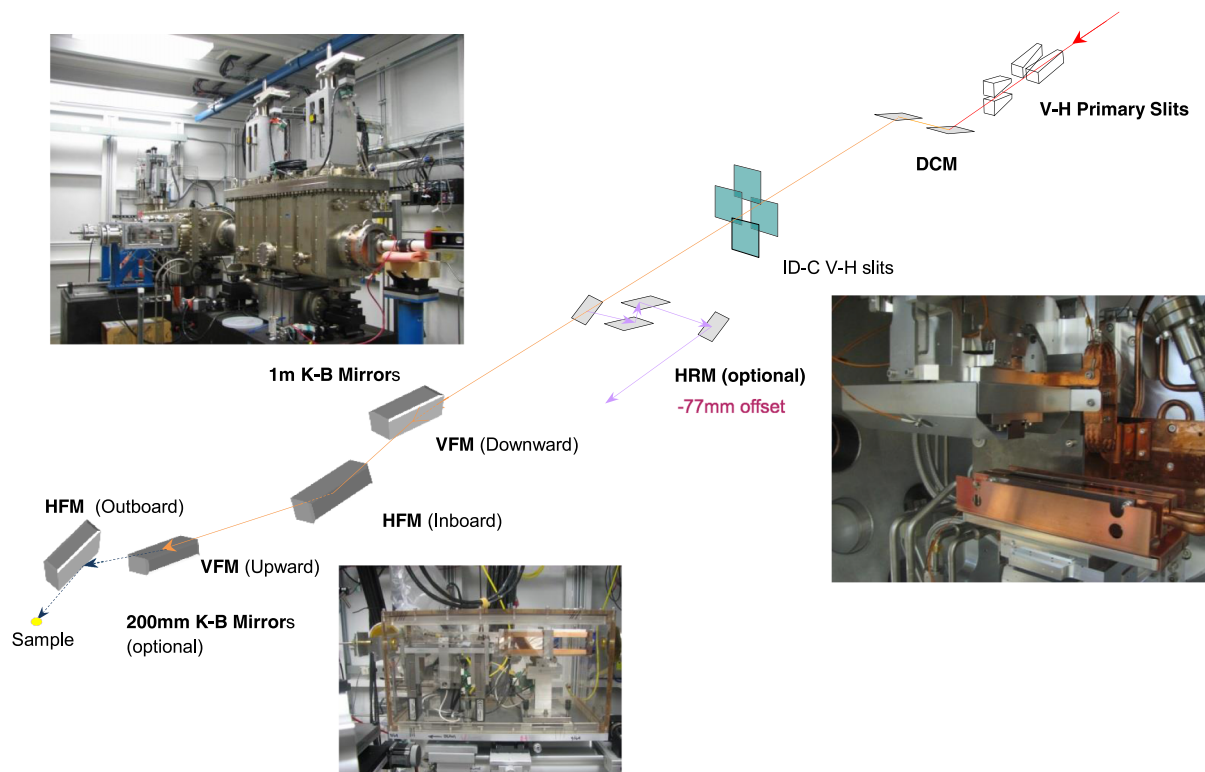
FIG. 1. Schematic layout of the high pressure X-ray spectroscopy beamline at HPCAT. From right to left: vertical and horizontal primary slits; DCM, cryo-cooled double crystal Si (1 1 1) monochromator; IDC V-H slits; HRM (optional), high resolution monochromators for ^{57}Fe NRS experiments; meter long KB mirrors, 200 mm KB mirrors (optional for 3(V) × 5 (H) μm^2 focus), and sample. Inset pictures are IDC hutch with meter long KB mirrors (top left), 200 mm KB mirrors in IDD (bottom), and DCM (right).

FIG. 2. Available focus profiles at the sample position. Focus with (a) both large KB mirrors; (b) vertical large, horizontal 200 mm KB mirrors; (c) vertical 200 mm, horizontal large KB mirrors; (d) both 200 mm KB mirrors (red bar in all pictures is 10 μm); (e) and (f) sharp edge scans of vertical and horizontal directions showing $\sim 3 \times 5$ μm FWHM focus with 200 mm KB mirrors.

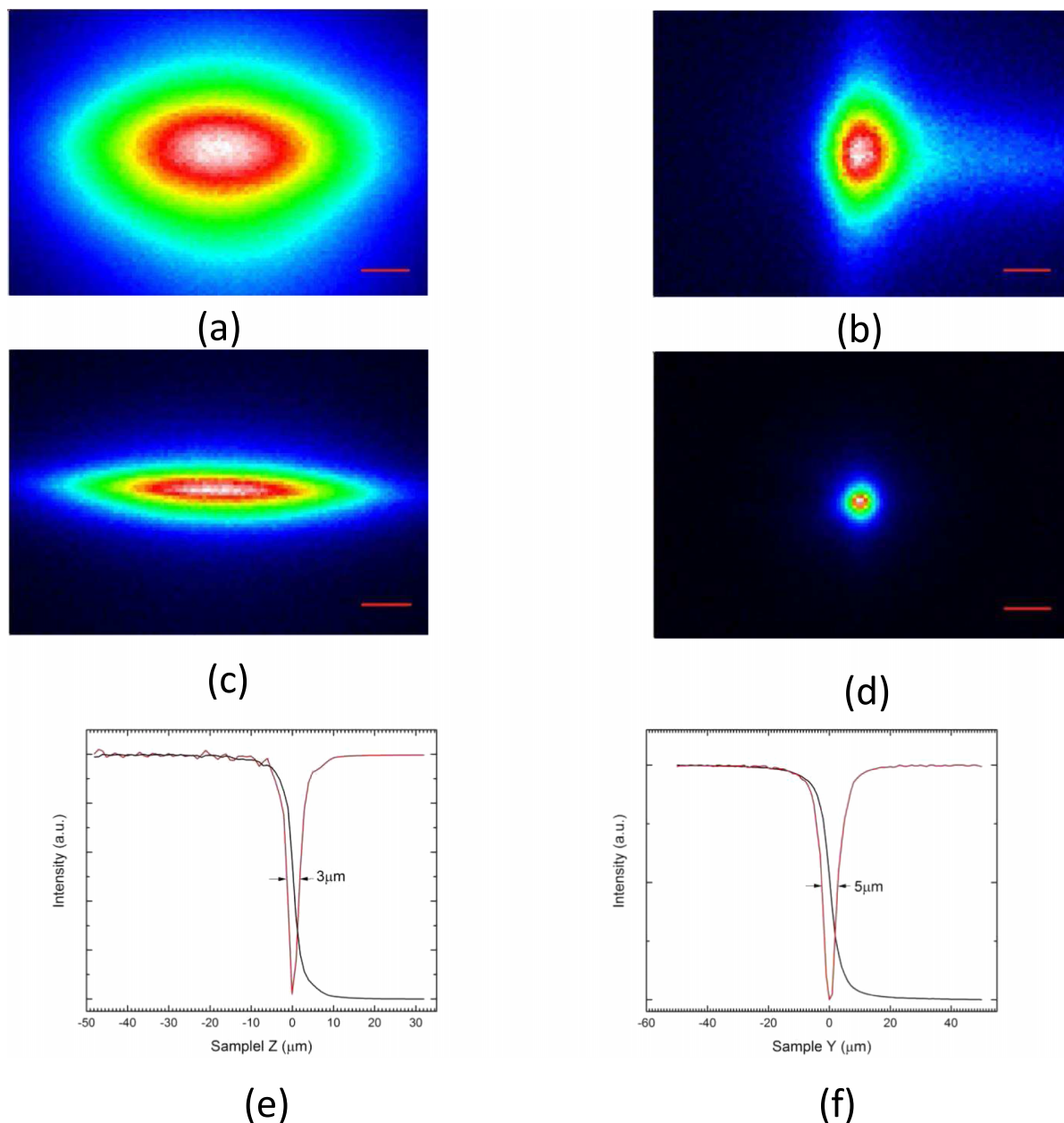the core hole is filled by an electron from a higher shell. Another photon, whose energy equals the energy difference between the two electronic levels, is emitted. XES can provide valence, spin, and bond information of the system studied. Since its first application under high pressure in the late 1990s, XES has been widely used to study the behavior of materials under high pressure.[13–16] Using the same experimental setup, resonant X-ray emission spectroscopy (RXES) and partial fluorescence yield X-ray absorption spectroscopy (PFY-XAS) experiments can be performed at various incident energies across the absorption edge. During RXES experiments, X-ray emission spectra are collected for different selected incident energies near an absorption edge. RXES studies of transition-metal and rare-earth systems give us important information on the electronic states of the sample systems, such as the

intra-atomic multiplet coupling, electron correlation, and inter-atomic hybridization.[17–19]

In our current XES setup (Figure 3(a)), an emission spectrum is collected by a one-meter Rowland circle spectrometer in the vertical scattering geometry. The XES spectrometer uses a four-inch bent silicon analyzer to spectrally analyze the fluorescence from the sample and reflects it to a Peltier-cooled silicon detector (Amptek XR 100CR). The analyzer is made by gluing a single-crystal Si wafer onto a spherically ground concave glass substrate of one-meter radius (NJ-XRS Tech). With one analyzer, the spectrometer covers a solid angle of $\sim$8 msr. For different emission energies, the Rowland condition is achieved by adjusting the distances between analyzer and sample, and analyzer and detector, respectively. Both analyzer and detectors are mounted on rotation
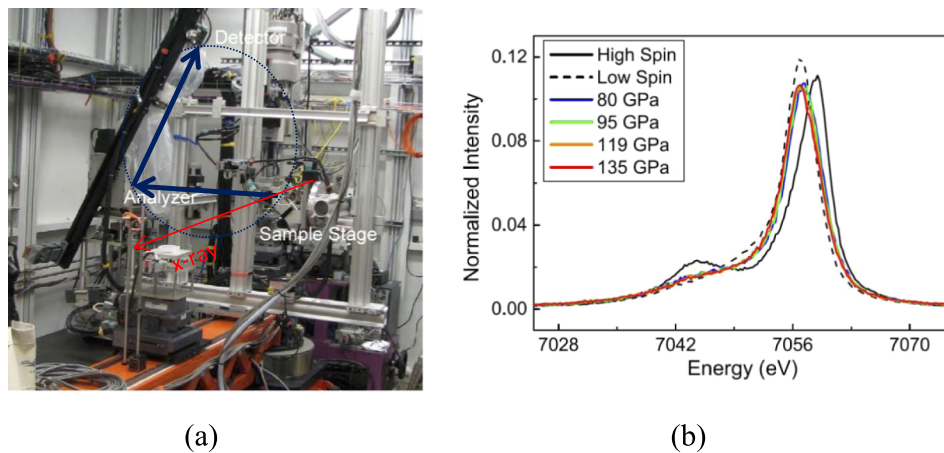
FIG. 3. (a) Current X-ray emission spectrometer at 16 ID-D. Sample, analyzer, and detector are shown in the 1-m Rowland circle. (b) Fe K_β XES spectra of perovskite (Pv25) up to 135 GPa (adapted from Fig. 3 of Mao *et al.*).[40]

stages which rotate in vertical plane and have 0.001° resolution. The analyzer stage also can be rotated in horizontal plane to steer the fluorescence signal into the detector. An emission spectrum is obtained by rotating the analyzer $\Delta\vartheta$, tracked by the corresponding $2\Delta\vartheta$ rotation of the detector. The emission energy is calibrated using a standard foil or a material containing the target emission element located at the sample position. The energy resolution of the spectrometer depends on the intrinsic energy resolution of the analyzer and geometrical contributions. The overall energy resolution of our XES ranges from ~0.5 to 2 eV. In order to reduce the scattering background, the analyzer is set perpendicular to the incident beam. For high pressure XES experiments with DACs, a beryllium gasket is mostly used. Normal Be gaskets contain trace amounts of impurities such as Cu and Fe (e.g., it may contain 0.05% Fe). Special attention needs to be taken to avoid contribution to the signal from impurities in Be gasket. Focused beam sizes should be smaller than the sample size, and if the measurements are for elements of Fe and Cu, ultrapure Be gasket or other x-ray transparent materials should be used.

Fig. 3(b) shows the XES spectra of Fe $K_{\beta1,3}$ of iron-rich silicate perovskite up to 135 GPa. The sample ($Mg_{0.75}Fe_{0.25}$) SiO_3 (Pv25) was loaded in a DAC with a pre-indented Be gasket and cBN gasket insert. Sample size is about 50 μm in diameter. The XES spectra were collected at 80, 95, 119, and 135 GPa. Combining XRD and nuclear forward scattering (NFS) results showed that an increase in density and bulk sound velocity of Pv25 can be explained by the occurrence of the low-spin Fe^{3+} and the extremely high-quadrupole component of Fe^{2+}. A range of emission lines (4.5-22 keV) can be studied by selecting proper Si analyzers. A list of current available Si analyzers and emission lines and corresponding Bragg angles is summarized in Table II. Generally the largest possible Bragg angle for each emission line is used for better energy resolution. However, due to space constraints from helium flight paths and cryostats, sometimes we need to select an analyzer with a smaller Bragg angle. To be able to expand the temperature range of XES experiments to the low temperature region, we have developed a new cryostat which can reach down to ~10 K for R/XES studies on magnetic properties

and spin transitions of many functional materials under high pressures and low temperatures.[19,20]

To improve the efficiency of the XES experiments, we have used both a miniature x-ray emission spectrometer (miniXES) and an X-ray polycapillary lens for improving signal/noise ratio in data collection. The miniXES contains a few small flat crystals which are placed close to the sample and arranged in Johansson geometry, together with a spatial filtering aperture and a low-noise x-ray position sensitive detector (Pilatus100K is used currently).[21] Due to its close proximity to the sample, a large solid angle of XES signal can be collected. Another method to increase the collected solid angle is the use of a polycapillary optic.[22] The polycapillary half-lens we use in our XES was designed and manufactured by XOS, Inc. It has a focus length ~8.5 mm, input focus spot ~50 μm, and 16° collection angle. The transmission efficiency measured at 8 keV is ~22%. A flat crystal is used as an analyzer for the output quasi-parallel beam (~8 mm in size)

TABLE II. Analyzers available at HPCAT with measured emission lines including Bragg angle.

Analyzer	Emission lines with energy (in keV) and Bragg angles
Si (100)	Ce $L_{\alpha1}$ 4.84 (70.613°), Pr $L_{\alpha1}$ 5.034 (65.099°), Cr $K_{\alpha1}$ 5.415 (57.481°), V $K_{\beta1,3}$ 5.427 (57.273°), Sm $L_{\alpha1}$ 5.636 (54.105°), Tb $L_{\gamma1}$ 8.102 (77.44°), Cu $K_{\beta1}$ 8.905 (62.626°), Ga $K_{\alpha1}$ 9.252 (80.752°), Au $L_{\alpha1}$ 9.713 (70.069°), Se $K_{\alpha1}$ 11.222 (61.744°), Pu $L_{\alpha1}$ 14.279 (73.594°)
Si (111)	Ce $L_{\gamma1}$ 6.052 (78.527°), Pr $L_{\gamma1}$ 6.322 (69.743°), Fe $K_{\alpha1}$ 6.404 (67.846°), Mn $K_{\beta1,3}$ 6.49 (66.038°), Ga $K_{\beta1}$ 10.265 (74.38°), Ge $K_{\beta2}$ 11.101 (62.935°)
Si (110)	Nd $L_{\gamma1}$ 6.602 (77.963°), Sm $L_{\gamma1}$ 7.178 (64.099°), Fe $K_{\beta1,3}$ 7.058 (66.183°), Hg $L_{\alpha1}$ 9.989 (75.843°), U $L_{\alpha1}$ 13.615 (71.536°), U $L_{\gamma1}$ 20.167 (73.853°), Pu $L_{\gamma1}$ 21.417 (64.754°)
Si (422)	Eu $L_{\alpha1}$ 5.846 (73.054°), Mn $K_{\alpha1}$ 5.899 (74.437°), Cr $K_{\beta1,3}$ 5.947 (70.107°), Pu $L_{\beta5}$ 17.951 (69.162°)
Si (620)	Yb $L_{\alpha1}$ 7.415 (76.783°), Eu $L_{\gamma1}$ 7.48 (74.814°), Co $K_{\beta1,3}$ 7.649 (70.69°), Gd $L_{\gamma1}$ 7.786 (68.004°), Zr $K_{\beta1}$ 17.668 (54.806°), Nb $K_{\beta1}$ 18.622 (60.091°)

from the half-lens and a Pilatus100k collects the diffracted beam.

Both miniXES and the polycapillary XES improve experimental efficiency by a factor of 5-10.[21,22] However, every miniXES is specifically designed for only one emission line and data analysis is not trivial for general users (energy calibration for each individual pixel of the position sensitive detector and image processing). For very dilute samples under Mbar pressure with very low count rate, background may become an issue for the image processing. For our XES with polycapillary half-lens, the energy resolution is ~5-10 eV. That is suitable for studies of 2p excitation of lanthanides because the core-hole lifetime broadening of the excitation is about 4-5 eV. We are in the process of building a multi-analyzer XES which can collect a similar solid angle compared to miniXES and polycapillary lens spectrometer and still keep the energy resolution at ~1 eV. The preliminary design is shown in Figure 4. The spectrometer will have seven 4-in. spherical bent analyzers arranged in a hexagonal pattern to make it compact and accommodate the opening of the most used 2-in. symmetric diamond anvil cells.

B. High pressure inelastic x-ray scattering

IXS has become a powerful tool to study lattice and electronic excitations in condensed matter physics.[8] Presently, HP-CAT has a spectrometer for the study of electronic excitations at low momentum transfer and core-electron excitations (X-ray Raman scattering (XRS)) at larger scattering angle with ~1 eV energy resolution. The spectrometer is designed to detect scattered photons of energies of interest with an energy resolution and momentum transfer corresponding to the physics process of interest. XRS yields information on the bonding of electrons and the electronic structure (energy levels and occupation of orbitals).[23–26] The geometry of scattering can be selected to probe different bonding directions, for example, in layered materials.[27] If the photon energy-loss is on the order of a fraction of eV to tens of eV, one can study valance excitations, plasmons (collective excitations of the electron gas), and their dispersions with small momentum transfer.[28,29]

The main challenge in the use of the IXS technique with DACs comes from both the low-counting rate because of small scattering cross section and small sample size under high pressure and from background scattering produced by the gasket and diamonds enclosing the sample. For a beamline doing high pressure IXS experiments, collecting as much X-ray flux as possible, and focusing the beam to a size smaller than that of the sample to reduce illumination on the area outside of the sample are very important.

During an IXS experiment, the incident beam hits the sample; scattered x-rays are collected by spherically bent single-crystal analyzers and focused to the solid state detector in a nearly backscattering geometry. To improve the solid angle for data collection, a 17-element analyzer array has been developed and installed at 16-ID-D. The array, which is shown in Figure 5(a), consists of three columns of 2-in. diameter bent silicon (111) analyzers from NJ-XRS Tech in a vertical Rowland circle backscattering geometry. The radius of these bent analyzers is 1 m. The 17-element analyzer array covers a solid angle of ~34 msr. The distance between sample and detector (Amptek XR 100CR) is fixed at 50 mm, with a backscattering angle at 87.7°. The elastic energy is 9.886 keV using the Si (5 5 5) reflection. The alignment of the spectrometer is done by putting a 100 μm diameter glass fiber as the scattering source at the sample position. The two-theta (2ϑ) angle is set
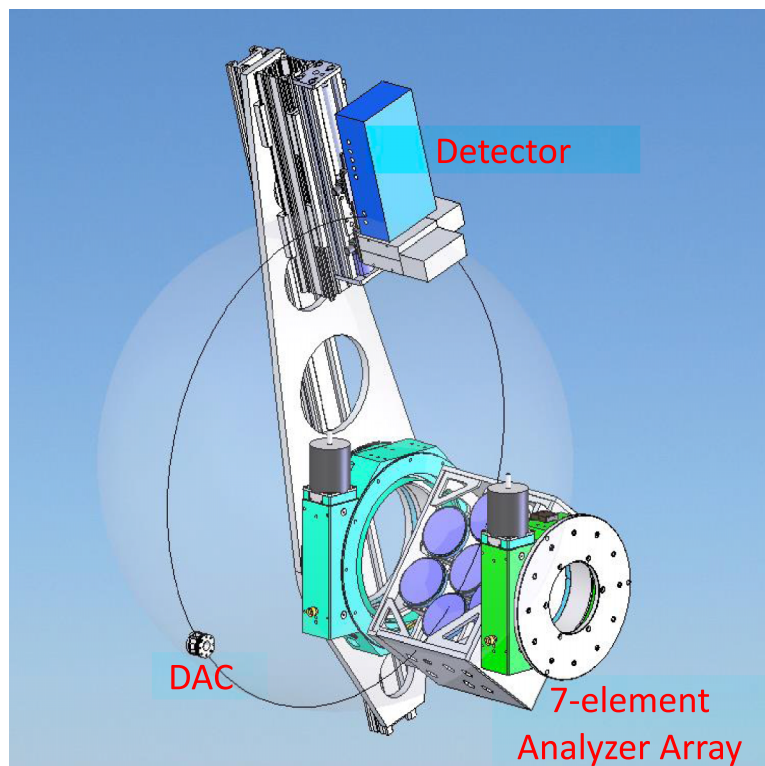

FIG. 4. Design of a XES with 7-element analyzer.

at 18.3° to get maximum elastic scattering. When detecting an elastic scattering signal, the detector position is optimized by scanning in both the vertical and horizontal directions. The IXS signals are collected by changing or scanning the incident x-ray energy relative to the elastic line. The overall energy resolution of the IXS spectrometer is ~1.2 eV. Momentum dependent spectra can be obtained by varying the 2ϑ angle of the spectrometer arm. Accessible range of scattering angle of our IXS spectrometer is 0°-90°. Because the polarization of

X-rays at APS is in vertical direction and our IXS spectrometer rotates in horizontal plane, the IXS signal becomes weaker with increasing in 2ϑ angle. Background forward scattering increases with decreasing 2ϑ angle. Considering these two effects together, for q-integrated IXS, 2ϑ angle is usually set around 30° to get the best signal-to-noise ratios. In Figure 5(b), Na plasmon up to 87 GPa measured with different momentum transfers q is shown. Three sets of diamond anvils were used to optimize the trade-off between sample size and pressure range.
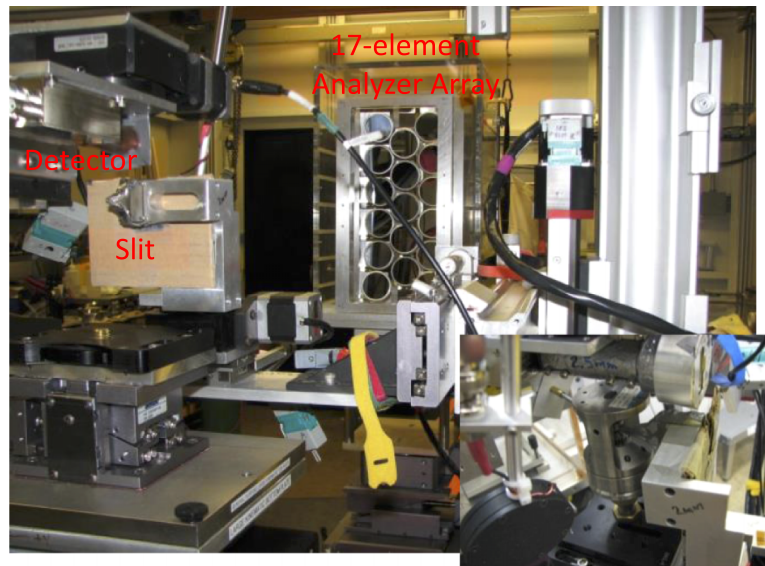
(a)
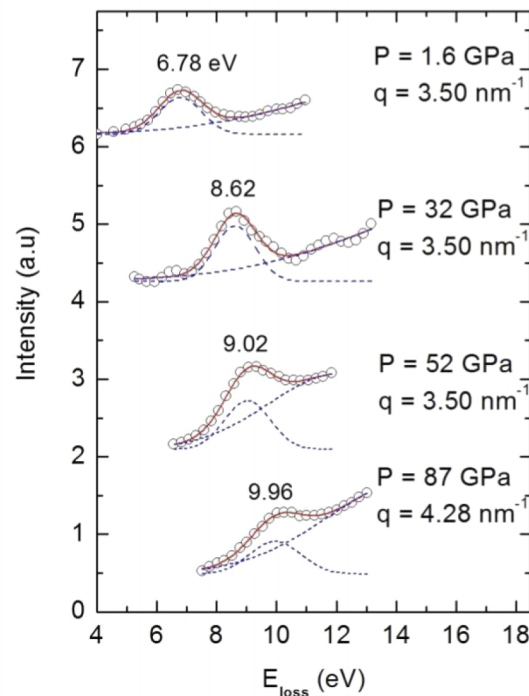
(b)

FIG. 5. (a) 17-element Si (1 1 1) analyzer array employed in backscattering geometry for inelastic X-ray scattering. The inset shows sample environment during experiment. (b) Na plasmon up to 87 GPa measured with different q.

A pair of diamond anvils with 500 μm culet diameter were used for experiments up to 32 GPa; 400 μm culet, up to 52 GPa; and 200 μm culet with 10° bevel to an outer diameter of 400 μm, to 97 GPa. The sample chamber sizes were 170, 130, and 100 μm for the culet size of 500, 400, and 200 μm (beveled), respectively. Experimental data showed that the solid Na of both bcc and fcc symmetries can be regarded as simple metals even under multiple fold densification.

In addition to a small focus beam size, post-sample collimation is critical for high pressure IXS experiments. A slit or double slit system is used traditionally.[30] At HPCAT, we are currently using a tweezers slit as shown in Figure 5(a). To achieve background scattering rejection, the slit needs to be put as close as possible to the sample and a paranomic DAC with large open angle is often used due to ease of access. In recent years, we started to use a full polycapillary lens as post-sample collimation. This collimator allows for large solid angle collection and minimum background scattering from other DAC components (diamond anvils, Be gasket, etc.) due to the focusing capability of the polycapillary lenses. Although the polycapillary efficiency at 10 keV is ~15%, the confocal geometry improves the signal-to-noise ratio, especially for studies of electronic excitations close to the elastic line. Another advantage of using a polycapillary lens is that a multi-analyzer system approach is not necessary due to the beam coming out from the polycapillary being focused down to ~100 μm and the exit cone angle is ~2.5°. The details and experimental results of polycapillary IXS developments are presented in Ref. 12.

C. High pressure nuclear resonant scattering

The NRS technique has been widely used to study biomolecules, thin films, and materials under extreme conditions in recent years.[31] The NRS technique is selective for particular isotopes. Only samples with resonant nuclei contribute to the signal. This isotope selectivity is very helpful for high pressure

studies by suppressing the background signals, where samples are normally enclosed by surrounding materials (gasket, diamond, etc.).

NRS can be divided into two methods: nuclear resonant inelastic X-ray scattering (NRIXS) and NFS. NRIXS is a technique in which energy gain or loss through a scattering process involving phonon excitations is monitored or recorded via excitation of a Mössbauer resonance. Apart from the familiar "zero phonon" Mössbauer resonance which NFS is based on, there are additional transitions that correspond to nuclear excitation in combination with excitation (Stokes) or de-excitation (anti-Stokes) of phonon modes. From NRIXS, the partial density of states (pDOS) can be obtained to derive important dynamic, thermodynamic, and elastic information such as vibrational kinetic energy, vibrational entropy, Debye temperature, and sound velocities. From NFS, hyperfine interaction parameters can be obtained to give information on spin state, oxidation state, and magnetic ordering.

^{57}Fe NRS has attracted particular attention among physicists and geophysicists because Fe is an archetypal transition element and is a dominant component in the cores of the earth and other terrestrial planets. At HPCAT, a 2.2-meV HRM is used for ^{57}Fe NRS experiments. The HRM consists of 2 channel-cut silicon crystals [Si(4 4 0) and Si (9 7 5)] (Figure 6(a)).

During NRS experiments, the bandwidth of the undulator beam is reduced to ~1.5 eV by the liquid N_2 cooled Si DCM in 16 ID-A. After going through the HRM in IDC (Insertion Device - C station), the bandwidth of the X-ray beam is further reduced to ~2.2 meV. The highly monochromatic x-ray beam is tuned to ^{57}Fe nuclear resonance at 14.413 keV and is then focused by KB mirrors before hitting the sample. Using time discrimination electronics and fast avalanching photo diodes (APDs), NRS signals are collected by one APD in the forward direction for NFS measurements or multiple APDs around the sample for NRIXS measurements.
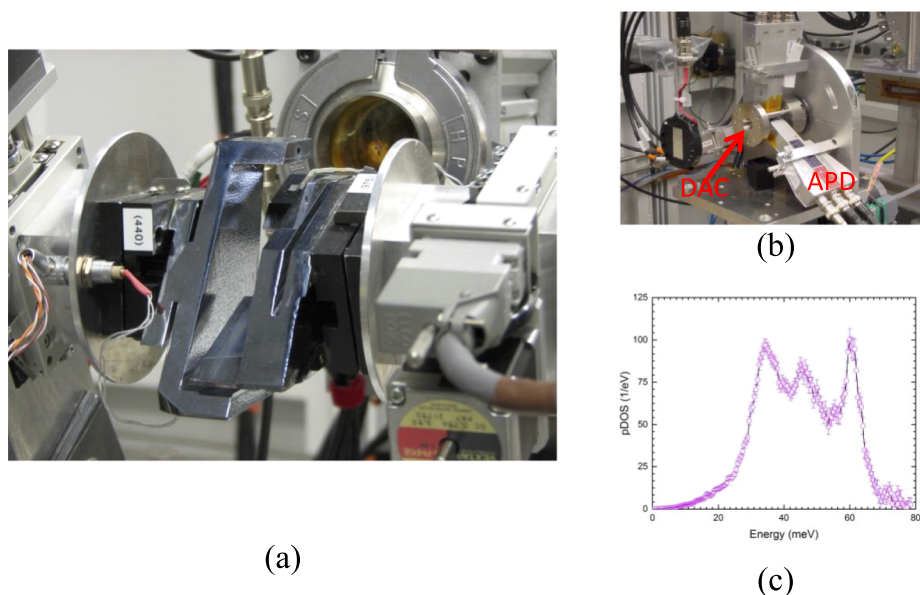

(a)

(b)

(c)

FIG. 6. (a) Photograph of the ~2 meV high resolution monochromator for ^{57}Fe nuclear resonant scattering experiment. (b) Photograph of high pressure NRIXS setup at 16 ID-D, 3 APD detectors are put close around a panoramic diamond anvil cell. (c) Fe pDOS data measured at 136 GPa.

Although only the ^{57}Fe enriched sample gives NRS delay signals, a small focused beam size is still critical for high pressure NRS experiments due to small sample size. For NFS experiments, a small beam size can also reduce effects caused by sample inhomogeneity. To improve the collection solid angle for weak NRXIS signals, multiple APDs are put as close as possible to the sample. Special twofold or triple-fold DACs were designed to accommodate 2 or 3 APDs with 10 mm^2 active area that can be put a few millimeters away from sample as shown in Fig. 6(b). We have two cryostats for low temperature NFS experiments (details about those cryostats are presented by Sinogenkin *et al.* in same issue). Both cryostats can be coupled to a membrane pressure control system to change pressure at low temperature and an on-line Ruby system to measure pressure *in-situ*.

Because of the isotope selectivity of NRS and unique properties of synchrotron radiation: high brightness, highly linearly polarized, and small beam size, NRS is particularly suitable for high pressure research compared to conventional Mössbauer spectroscopy using a radioactive source. Several beamlines specialized in NRS techniques (3-ID at APS, 18-ID at ESRF (European Synchrotron Radiation Facility), and 9-ID at SPring-8) have high pressure research activities.[32,33] At 16 ID-D of HPCAT, Mbar pressure NRS experiments are often performed. Figure 6(c) shows pDOS of Fe measured at 136 GPa.[34] For Mbar pressure NFS experiments, the collection time for ^{57}Fe enriched Fe-alloy and oxides sample is typically ~30 min; for low Fe-content silicate perovskite samples, collection time can be 2-4 h.

Nuclear resonant scattering experiments require not only the high brilliance of a synchrotron and a meV bandwidth high resolution monochromator but also a suitable time structure of the synchrotron. To distinguish the NRS signal from other much stronger electronic scattering, fast time discrimination electronics and an APD (~ns temporal resolution) are used. Because the NRS signal decays normally in tens or hundreds of nanoseconds, a large time separation between synchrotron pulses is desired, especially for nuclear forward scattering experiments. All NRS experiments done at HPCAT use APS 24-bunch mode that has a 153 ns time separation between two synchrotron pulses. Recently, the diffraction-limited storage ring (DLSR) concept has been demonstrated to be feasible for large storage ring like APS, ESRF, and SPring-8 in addition to smaller diameter rings already being built such as MAX-IV in Sweden and SIRIUS in Brazil.[35] From the initial design parameters of the new APS multi-bend achromatic (MBA) ring,[36] the largest time separation will be ~76 ns which does not significantly impact NRS experiments of isotopes with a few tens of ns half-life like Eu, Sn, and Sm. For the most commonly measured NRS isotope ^{57}Fe which has 141 ns half-life, this time separation is still good enough for NRIXS experiments which integrate signals from the entire time-collection window. However, for NFS experiments, the 76 ns time window is too short to collect useful time spectra. To overcome the short time window and efficiency loss due to HRM, a high-speed shutter near the focus spot of a micro-focused beam can be used. Measurements have been done at the APS with a 1 kHz high speed shutter to prove the principle.[37] Without a high speed shutter, a HRM is needed to reduce bandwidth of the incoming beam to meV level in order not to saturate the forward APD detector with direct beam. Incident beam intensity is reduced ~500-1000 times by the HRM. With improving high-speed shutter technology and smaller focus beam, a factor of ~1000 improvement in collecting efficiency is possible.

IV. OPTIMIZATION AND INTEGRATION

All three techniques mentioned above require high incident flux and a large collection solid angle due to small scattering cross sections. At 16 ID-D, we provide different focus sizes to match different experiment requirements. Most experiments use 30 (V) × 50 (H) μm^2 due to flux requirements. The smallest beam we can provide now is 3 (V) × 5 (H) μm^2 using 200 mm KB mirrors. We will soon have 320 mm (H) × 400 mm (V) KB mirrors for 3 (V) × 5 (H) μm^2 with on-sample flux comparable to that from the current 30 (V) × 50 (H) μm^2. To fulfill some experiments with even smaller beam size requirements, we are working with the APS optics group to develop pre-figured mirrors to achieve 1 (V) × 2 (H) μm^2 with ~5% flux compared to beam using the long KB mirrors.

One unique feature of 16 ID-D of HPCAT is the multiple techniques available for high pressure x-ray spectroscopy studies. Materials under high pressure can be studied using different techniques to get a comprehensive understanding. For example, both XES and NRS techniques have been used to study the iron based superconductor FeSe at 16 ID-D,[20,38] although these two experiments were done at different times due to the special requirements of NRS (meV resolution X-ray beam, etc.). XES and IXS techniques can also be integrated to get complementary properties of samples under the same conditions. This integration approach is especially useful for samples that are difficult to synthesize or sensitive to specific stress conditions. However, different techniques require different beamline configurations, such as incoming energy and focus size, to be optimized, performance for one technique may be compromised under integration approach. Another practical concern is that data collection for high pressure spectroscopic measurements usually takes long hours. Combining two spectroscopic techniques together may take substantial beamtime, which can be very competitive. For samples whose structures are sensitive to small pressure or temperature changes during data collection, *in-situ* XRD becomes useful. We have integrated *in-situ* XRD using a MarCCD with XES, NFS, and X-ray fluorescence spectroscopy (XFS) at HPCAT.[39] The incident X-ray energy for XES techniques is low for high pressure XRD experiments (normally we set the incident energy at 11.3 keV for non-resonant XES, and high pressure XRD experiments prefer incoming energy above 20 keV). To combine XES and XRD together right now, we need to select incident energy around 20 keV which has less flux compared to 11.3 keV. We plan to change the beamline design to be able to change incident energy easily without changing the beam focus spot. In the future, XES and NRS experiments integrated with *in-situ* XRD will become more routine at 16 ID-D.

In conclusion, we have developed three types of x-ray spectroscopy techniques (XES, IXS, and NRS) at 16 ID-D of HPCAT at the APS, suitable for high pressure research. These

techniques can be integrated with *in-situ* X-ray diffraction, which provide a platform for studying materials' electronic, magnetic, and structural properties under high pressure. In addition to high pressure devices, cryostats, and furnaces, the beamline is equipped with on-line pressure control and measurement systems. The future developments include maximizing on-sample flux, sub-micron beam size, and efficient collimation to further suppress the unwanted signals from surrounding materials.

ACKNOWLEDGMENTS

[1] M. H. Manghnani, L. C. Ming, and J. C. Jamieson, Nucl. Instrum. Methods **177**, 219 (1980).

[2] V. V. Struzhkin, R. J. Hemley, H. K. Mao, Y. A. Timofeev, and M. I. Eremets, Hyperfine Interact. **128**, 323 (2000).

[3] P. F. McMillan, Chem. Soc. Rev. **35**, 855 (2006).

[4] W. A. Bassett, Phys. Earth Planet. Inter. **23**, 337 (1980).

[5] D. M. Adams, A. E. Heath, M. Pogson, and P. W. Ruff, Spectrochim. Acta, Part A **47**, 1075 (1991).

[6] R. J. Hemley, H. K. Mao, and V. V. Struzhkin, J. Synchrotron Radiat. **12**, 135 (2005).

[7] T. S. Duffy, Rep. Prog. Phys. **68**, 1811 (2005).

[8] H. K. Mao, C. C. Kao, and R. J. Hemley, J. Phys.: Condens. Matter **13**, 7847 (2001).

[9] D. Haskel, Y. C. Tseng, N. M. Souza-Neto, J. C. Lang, S. Sinogeikin, Y. Mudryk, K. A. Gschneidner, Jr., and V. K. Pecharsky, High Pressure Res. **28**, 185 (2008).

[10] G. Shen and Y. Wang, Spectrosc. Methods Mineralology Mater. Sci. **78**, 745 (2014).

[11] G. Shen, P. Chow, Y. Xiao, S. Sinogeikin, Y. Meng, W. Yang, H.-P. Liermann, O. Shebanova, E. Rod, A. Bommannavar, and H.-K. Mao, High Pressure Res. **28**, 145 (2008).

[12] P. Chow, Y. M. Xiao, E. Rod, L. G. Bai, G. Y. Shen, S. Sinogeikin, N. Gao, Y. Ding, and H.-K. Mao, Rev. Sci. Instrum. **86**, 072203 (2015).

[13] J. P. Rueff, C. C. Kao, V. V. Struzhkin, J. Badro, J. Shu, R. J. Hemley, and H. K. Hao, Phys. Rev. Lett. **82**, 3284 (1999).

[14] L. Jung-Fu, A. G. Gavriliuk, V. V. Struzhkin, S. D. Jacobsen, W. Sturhahn, M. Y. Hu, P. Chow, and Y. Choong-Shik, Phys. Rev. B: Condens. Matter Mater. Phys. **73**, 113107 (2006).

[15] M. J. Lipp, A. P. Sorini, J. Bradley, B. Maddox, K. T. Moore, H. Cynn, T. P. Devereaux, Y. Xiao, P. Chow, and W. J. Evans, Phys. Rev. Lett. **109**, 195705 (2012).

[16] C.-S. Yoo, B. Maddox, and V. Iota, in *Actinides 2008-Basic Science, Applications and Technology*, edited by D. K. Shuh, B. W. Chung, T. AlbrechtSchmitt, T. Gouder, and J. D. Thompson (Cambridge University Press, 2008), Vol. 1104, p. 3.

[17] J.-F. Lin, Z. Mao, I. Jarrige, Y. Xiao, P. Chow, T. Okuchi, N. Hiraoka, and S. D. Jacobsen, Am. Mineral. **95**, 1125 (2010).

[18] R. S. Kumar, A. Svane, G. Vaitheeswaran, V. Kanchana, E. D. Bauer, M. Hu, M. F. Nicol, and A. L. Cornelius, Phys. Rev. B **78**, 075117 (2008).

[19] R. S. Kumar, Y. Zhang, A. Thamizhavel, A. Svane, G. Vaitheeswaran, V. Kanchana, Y. Xiao, P. Chow, C. Chen, and Y. Zhao, Appl. Phys. Lett. **104**, 042601 (2014).

[20] R. S. Kumar, Y. Zhang, Y. Xiao, J. Baker, A. Cornelius, S. Veeramalai, P. Chow, C. Chen, and Y. Zhao, Appl. Phys. Lett. **99**, 061913 (2011).

[21] J. I. Pacold, J. A. Bradley, B. A. Mattern, M. J. Lipp, G. T. Seidler, P. Chow, Y. Xiao, E. Rod, B. Rusthoven, and J. Quintana, J. Synchrotron Radiat. **19**, 245 (2012).

[22] D. R. Mortensen, G. T. Seidler, J. A. Bradley, M. J. Lipp, W. J. Evans, P. Chow, Y. M. Xiao, G. Boman, and M. E. Bowden, Rev. Sci. Instrum. **84**, 083908 (2013).

[23] Y. Meng, H. K. Mao, P. J. Eng, T. P. Trainor, M. Newville, M. Y. Hu, C. C. Kao, J. F. Shu, D. Hausermann, and R. J. Hemley, Nat. Mater. **3**, 111 (2004).

[24] R. S. Kumar, M. G. Pravica, A. L. Cornelius, M. F. Nicol, M. Y. Hu, and P. C. Chow, Diamond Relat. Mater. **16**, 1250 (2007).

[25] S. K. Lee, P. J. Eng, H. K. Mao, Y. Meng, M. Newville, M. Y. Hu, and J. F. Shu, Nat. Mater. **4**, 851 (2005).

[26] Y. Meng, P. J. Eng, J. S. Tse, D. M. Shaw, M. Y. Hu, J. Shu, S. A. Gramsch, C. Kao, R. J. Hemley, and H.-k. Mao, Proc. Natl. Acad. Sci. U. S. A. **105**, 11640 (2008).

[27] W. L. Mao, H. K. Mao, P. J. Eng, T. P. Trainor, M. Newville, C. C. Kao, D. L. Heinz, J. F. Shu, Y. Meng, and R. J. Hemley, Science **302**, 425 (2003).

[28] M. Ho Kwang, E. L. Shirley, D. Yang, P. Eng, Y. Q. Cai, P. Chow, X. Yuming, S. Jinfu, R. J. Hemley, K. Chichang, and W. L. Mao, Phys. Rev. Lett. **105**, 186404 (2010).

[29] H.-K. Mao, Y. Ding, Y. Xiao, P. Chow, J. Shu, S. Lebegue, A. Lazickif, and R. Ahuja, Proc. Natl. Acad. Sci. U. S. A. **108**, 20434 (2011).

[30] A. Alatas, H. Sinn, J. Zhao, A. H. Said, B. M. Leu, W. Sturhahn, E. E. Alp, G. Shen, and V. B. Prakapenka, High Pressure Res. **28**, 175 (2008).

[31] W. Sturhahn, J. Phys.: Condens. Matter **16**, S497 (2004).

[32] J. Y. Zhao, W. Sturhahn, J. F. Lin, G. Y. Shen, E. E. Alp, and H. K. Mao, High Pressure Res. **24**, 447 (2004).

[33] V. Potapkin, A. I. Chumakov, G. V. Smirnov, J.-P. Celse, R. Rueffer, C. Mccammon, and L. Dubrovinsky, J. Synchrotron Radiat. **19**, 559 (2012).

[34] A. E. Gleason, W. L. Mao, and J. Y. Zhao, Geophys. Res. Lett. **40**, 2983, doi:10.1002/grl.50588 (2013).

[35] R. Hettel, J. Synchrotron Radiat. **21**, 843 (2014).

[36] M. Borland, G. Decker, L. Emery, V. Sajaev, Y. Sun, and A. Xiao, J. Synchrotron Radiat. **21**, 912 (2014).

[37] T. S. Toellner, E. E. Alp, T. Graber, R. W. Henning, S. D. Shastri, G. Shenoy, and W. Sturhahn, J. Synchrotron Radiat. **18**, 183 (2011).

[38] R. S. Kumar, Y. Zhang, S. Sinogeikin, Y. Xiao, S. Kumar, P. Chow, A. L. Cornelius, and C. Chen, J. Phys. Chem. B **114**, 12597 (2010).

[39] E. A. Tanis, A. Simon, O. Tschauner, P. Chow, Y. Xiao, G. Shen, J. M. Hanchar, and M. Frank, Am. Mineral. **97**, 1708 (2012).

[40] Z. Mao, J. F. Lin, H. P. Scott, H. C. Watson, V. B. Prakapenka, Y. Xiao, P. Chow, and C. McCammon, Earth Planet. Sci. Lett. **309**, 179 (2011).